PAPER

Strain-inducing photochemical chlorination of graphene nanoribbons on SiC (0001)

Strain-inducing photochemical chlorination of graphene nanoribbons on SiC (0001)

Gabriela Copetti[1,2] ⓘ**, Eduardo H Nunes**[3]**, Taís O Feijó**[2,4] ⓘ**,
Lauren A Galves**[2]**, Martin Heilmann**[2] ⓘ**, Gabriel V Soares**[1,4] ⓘ**,
J Marcelo J Lopes**[2] **and Cláudio Radtke**[3,4,*] ⓘ

[1] Instituto de Física, UFRGS, 91501-970 Porto Alegre, Brazil
[2] Paul-Drude-Institut für Festkörperelektronik, Leibniz-Institut im Forschungsverbund Berlin e.V.,
D-10117 Berlin, Germany
[3] Instituto de Química, UFRGS, 90650-001 Porto Alegre, Brazil
[4] PGMICRO, UFRGS, 91501-970 Porto Alegre, Brazil

E-mail: claudio.radtke@ufrgs.br

CrossMark

Abstract

As different low-dimensional materials are sought to be incorporated into microelectronic devices, graphene integration is dependent on the development of band gap opening strategies. Amidst the different methods currently investigated, application of strain and use of electronic quantum confinement have shown promising results. In the present work, epitaxial graphene nanoribbons (GNR), formed by surface graphitization of SiC (0001) on crystalline step edges, were submitted to photochemical chlorination. The incorporation of Cl into the buffer layer underlying graphene increased the compressive uniaxial strain in the ribbons. Such method is a promising tool for tuning the band gap of GNRs.

Supplementary material for this article is available online

Keywords: graphene, nanoribbons, SiC, strain, chlorine, XPS, Raman

(Some figures may appear in colour only in the online journal)

1. Introduction

Its unique set of properties established graphene as a promising material for several technological applications. Reduced thickness and high electronic mobility make graphene especially interesting as channel material for transistors in high-performance devices [1–3]. However, the integration of graphene in such technologies is anything but trivial. CMOS-based logic depends on the 'off-state' electrical current being negligible compared to the 'on state' current. Since graphene possesses a zero-width band gap, the off state would not be achievable. To face this challenge, scientists have turned to band gap engineering. Tunable band gap can be achieved on bilayer graphene by application of an electric field [4]. On monolayer graphene, functionalization with adatoms such as F leads to band gaps as wide as 3 eV [5–8].

Strain applied to the graphene sheet was also shown to allow the increase of band gap width [9–13]. Finally, one dimensional quantum confinement in graphene has emerged as a promising method for opening the band gap: by reducing the lateral width of graphene to the <10 nm range, the number of allowed electronic states is decreased and the band gap is opened. Decreasing (or increasing) the physical width of these graphene nanoribbons (GNR) leads to the increase (or decrease) of the band gap width [14–17]. Band gap opening, significant enough so that GNR transistors with high on/off current ratio, has already been demonstrated [18, 19].

Reference [15] summarizes several methods used for producing GNR, which include lithography techniques, unzipping of carbon nanotubes, and direct growth on different substrates. The method used in the present work is epitaxial growth of GNRs on SiC (0001) [20, 21]. Graphitization of the SiC (0001) surface at high temperatures occurs at faster pace on SiC crystalline step edges. Therefore, stopping epitaxial

* Author to whom any correspondence should be addressed.
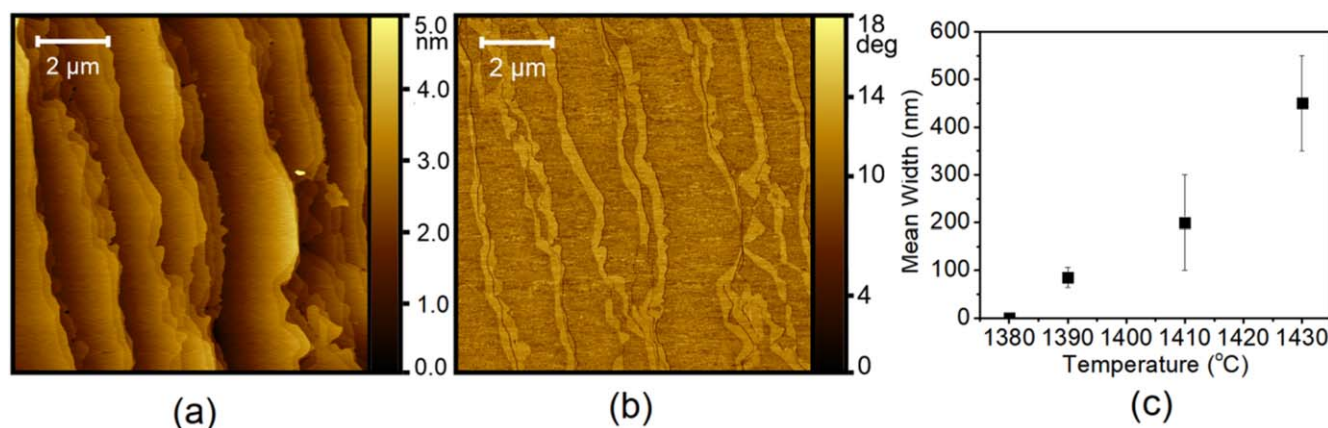
Figure 1. AFM (a) height and (b) phase images of graphene ribbons grown at 1410 °C. In (c), the mean width of the ribbons as a function of growth temperature is shown.

graphene growth in its initial stages yields GNR on such edges. The great advantage of this technique is the fact that it produces ribbons directly on an insulating substrate, with the possibility of attaining defect-free edges. These ribbons, however, tend to be relatively wide: several tenths of nm, which would lead to a minimal band gap. The use of artificial steps produced by lithography techniques should allow achieving a greater control over GNR growth [22], yielding narrower ribbons when compared to GNR growth performed on natural SiC step edges. Furthermore, synthesis of GNR on SiC can be combined with other band gap opening methods. For example, the production of quasi-free-standing bilayer GNR can be achieved upon O_2 intercalation of monolayer GNR grown on SiC [23, 24]. Therefore, methods to modify GNR are promising building blocks for developing band gap engineering of graphene.

In the present work, photochemical chlorination was used to modify GNR grown epitaxially on SiC (0001). Through Raman spectroscopy measurements, an increase in the uniaxial compressive strain applied to the GNR was observed to be not a result of chlorination of graphene itself, but a consequence of the modification of its substrate. Photochlorination led to Cl incorporation in the buffer layer (BL) that underlies graphene.

2. Methods

Prior to growth, SiC (0001) samples were chemically cleaned in n-Butyl acetate (10 min), acetone (5 min) and isopropanol (5 min) under ultrasound in order to remove the protective photoresist layer and any other organic residues. They are, afterwards, dipped in deionized water and dried with nitrogen gas. The samples are then placed in a RF inductive furnace and etched with forming gas (5 at% H_2 and 95 at% Ar) at 1400 °C in Ar flux of 500 sccm (900 mbar) for 15 min. This last procedure results not only on the removal of contaminants and surface imperfections, but also on the coalescence of SiC crystalline steps, that exist due to the wafer miscut.

The mechanism of GNR growth is described in [20]. In the present work, GNR were grown on the natural step edges

of SiC by annealing the samples within the 1390 °C–1430 °C range in an Ar flux of 100 sccm (900 mbar) for 15 min. Additionally, samples with complete graphene coverage were produced by increasing the temperature to 1600 °C and flux to 500 sccm. A BL, which also exhibits a honeycomb structure, but with about 1/3 of its C atoms covalently bonded to SiC, underlies the epitaxial graphene [25]. Reducing the temperature to 1380 °C (100 sccm, 900 mbar) leads to no graphene growth, but full coverage of the SiC surface with BL. To compare the effect of chlorination on graphene monolayer and bilayer, monolayer samples were heated in atmospheric air at 650 °C for 20 min to obtain quasi-free-standing bilayer graphene. The BL exposed to air is etched during annealing, while BL protected by the monolayer graphene decouples from the substrate, becoming a second graphene layer [23]. The annealing in air leads to the partial oxidation of the SiC surface.

Photochemical chlorination was performed submitting the samples to Cl_2 gas flow while exposing them to UV light from a mercury–xenon lamp at 80 W cm^{-2}. The Cl_2 gas was produced from the reaction $4HCl + MnO_2 \rightarrow Cl_2 + MnCl_2 + 2H_2O$. A N_2 flow leads the gaseous products to a balloon containing sulfuric acid, which retains the water vapor, before reaching the sample. Tapping mode atomic force microscopy (AFM) was used to study the surface morphology and determine the GNR lengths and widths through the analysis of height and phase-contrast. An Omicron-SPHERA station, with an Al-Kα x-ray source, was used to perform x-ray photoelectron spectroscopy (XPS) measurements to identify chemical bonding and composition prior and after chlorination. Raman spectroscopy, performed with 473 nm laser with 1 μm diameter spot and 600 g mm^{-1} grating, was used to observe strain modifications in graphene. Spectra were obtained in 12 × 12 μm^2 areas, with 1 μm distance between each measured point and 10 s integration. All Raman spectra shown are characteristic of the data set as a whole.

3. Results and discussion

Figures 1 (a) and (b) show AFM images of GNR grown at 1410 °C on natural steps-edges of SiC (0001). Raman spectroscopy was used to confirm that they were mainly constituted of monolayer graphene. Extracting the height profiles of several ribbons, the mean width was obtained (see supplementary information, available online at stacks.iop. org/NANO/32/145707/mmedia). At this growth temperature, it varied from 100 to 300 nm. The fixed growth time of 15 min was based on the time needed to synthesize a complete monolayer graphene using our experimental set-up at 1600 °C [23]. By changing the temperature (and keeping a 15 min growth time), we were able to confine the growth process to the region near to the step edge (to prepare GNRs). Though this range of width is too large for quantum confinement to occur, a decrease in the average width is possible by lowering growth temperature (figure 1(c)). Since greater graphene coverage yields a better signal-noise ratio in XPS and Raman analyses, wider GNR, such as the ones shown in figure 1, were used.

After GNR growth, the samples were submitted to photochemical chlorination. XPS spectra of monolayer GNR, before and after chlorination, are shown in figure 2. Prior to Cl incorporation, the signal present in the C 1s region could be deconvoluted into three components: C from the SiC substrate at 283.3 eV, C bonded to C at 284.4 eV, and C present in oxygenated contaminants (286.0, 287.7 and 288.8 eV). It is important to highlight that the XPS setup available did not allow the differentiation between C present in the BL and C present in the GNR. After chlorination, Cl incorporation is evident due to the appearance of the Cl 2s peak (271.4 eV). Additionally, an intense Cl 2p signal at 200.1 eV is seen in the survey spectrum (figure 2(a)). Interaction between Cl and C results in an intense binding energy shift at C 1s region (figure 2(b)). These components correspond to C–Cl (286.3 eV) and C-Cl$_2$ (288.4 eV). No changes were observed on the Si 2p region (data not shown). The GNR widths were measured once more after Cl incorporation, using AFM. It was verified that the average width was maintained and no sign of lateral corrosion was observable (data not shown).

Raman spectroscopy was used to investigate the effects of chlorination on GNR. Raman analyses provide various types of information on graphene, such as the number of layers, doping, and changes in mechanical strain [26–37]. After chlorination, a significant blueshift of the G and 2D peaks is observed (figure 3(a)). This blueshift is 5 times more intense for the 2D peak than for the G peak. Such proportion between the 2D and G peaks blueshifts has been shown to be associated with changes on the uniaxial strain applied to graphene [32]. While positive charge doping favors blueshift of the G peak, uniaxial compressive strain leads to a greater displacement of the 2D peak. Furthermore, an increase in doping would have led to a lowering of 2D∕G intensity ratio [31, 34, 35]. However, the exact opposite is observed. Another important evidence of strain-related effects is the widening of the G peak after chlorination. If the blueshift was
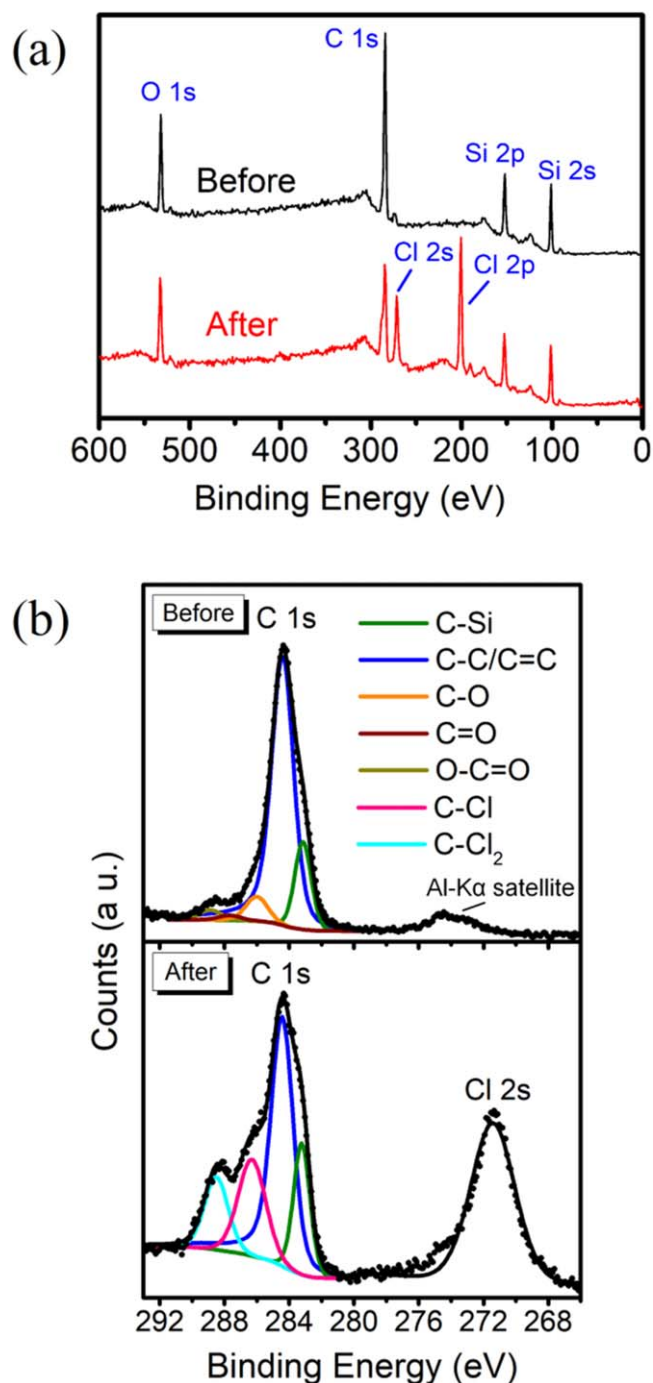
Figure 2. (a) XPS survey and (b) C 1s region of monolayer GNR sample before and after chlorination.

doping-related, the narrowing of the peak would occur [31, 34]. Wider G peaks, on the other hand, are associated to splitting caused by application of strain [30, 33]. Based on the cited literature, the observed shift of the Raman peaks indicates that chlorination mostly leads to strain. Ni *et al* [38] deposited graphene sheets on a transparent flexible substrate, which was stretched. Raman spectroscopy was used to study the strain effect on this layer. Significant red shift of the Raman 2D band ($\sim$27.8 cm^{-1} per 1% strain) for single-layer graphene was observed under the uniaxial tensile strain. In the same work, first-principle simulation of the band structure of
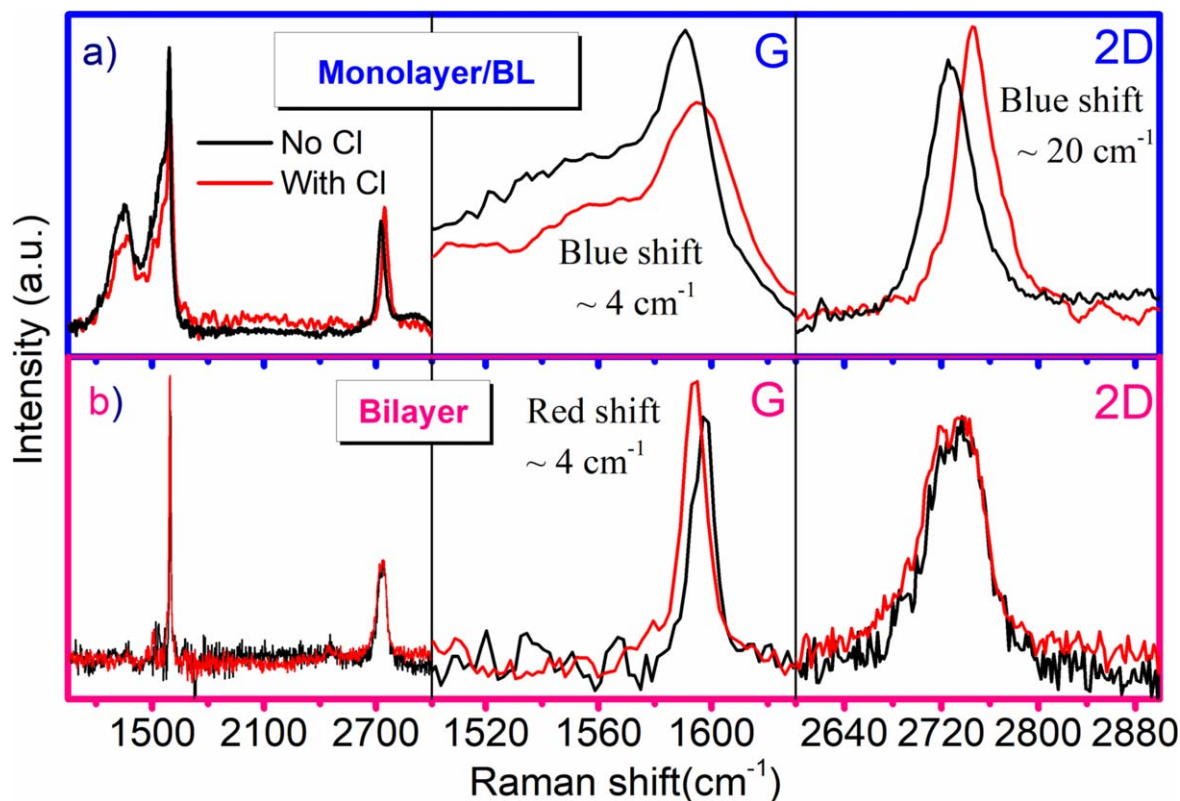
Figure 3. Raman spectra obtained with a 473 nm laser showing G and 2D peaks before and after chlorination for monolayer (a) and quasi-free-standing bilayer (b) GNR. As expected [23], the BL-related signal (D band) is absent in the spectra of the quasi-free-standing bilayer GNR sample which presents a sharper G signal as well. In addition, the full width at half maximum of the 2D peak increases from 33 cm^{-1} to 55 cm^{-1}, due to the conversion of monolayer to bilayer graphene in virtue of the decoupling of the BL. After chlorination, the G peak and the 2D peak of the monolayer GNR blueshift about 4 cm^{-1} and 20 cm^{-1}. For the bilayer GNR, a redshift of 4 cm^{-1} of the G peak occurs.

single-layer graphene shows a band-gap opening of 300 meV for 1% strain. Considering (i) the 20 cm^{-1} red shift in the 2D signal obtained in our samples following chlorination and (ii) results of [38], we estimated a band-gap opening of ~200 meV following GNRs chlorination.

In a previous study, doping of CVD-grown graphene on SiO$_2$ was observed after the same photochlorination process was used [35]. In this case, however, doping had a significantly different effect on the Raman spectra. Chlorine's high electronegativity led to p-type chemical doping. As expected, the blueshift of the G peak was more intense than that of the 2D peak, 2D/G intensity ratio decreased, and the G peak FWHM was reduced. Nevertheless, differences in the impact that chlorination has on the CVD-grown graphene transferred onto SiO$_2$ and epitaxial graphene on SiC were not unexpected. CVD-grown graphene possesses a higher defect density than epitaxial graphene and more surface contaminants are present due to the transfer process [39, 40], all of which may affect Cl incorporation. Furthermore, the underlying substrate has great influence on graphene [37, 41, 42]. Therefore, it is not surprising that graphene layers with different characteristics interact differently to chlorination. Nevertheless, the question remained whether Cl was in fact bonded to graphene or to the underlying substrate. To shed light on this problem, BL-only and fully covered graphene samples were chlorinated. One can observe in the
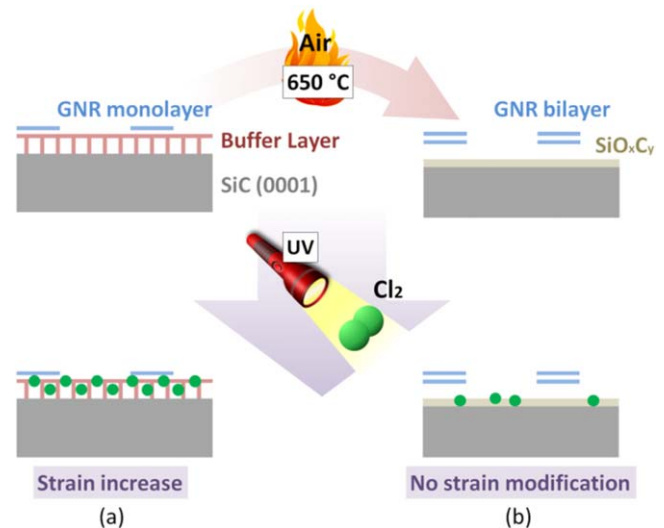
XPS spectra in figure 4(a) that the BL/SiC sample suffers drastic changes to its C1s signal after chlorination. On the other hand, chlorination led to a much less pronounced chemical displacement at the C 1s region for the graphene/BL/SiC sample (figure 4(b)). If epitaxial graphene was as reactive to photochlorination as the BL, the chemical displacement components should have the same proportion. This suggests that, while Cl can be easily incorporated into the BL, epitaxial graphene is much more inert to photochemical chlorination. The same scenario is observed while comparing the Cl amounts incorporated in a sample containing a BL with those of monolayer and bilayer GNRs (figure S2 of supplementary information). Sclauzero and Pasquarello have proposed that the bonding between the BL and SiC, which leads to a pyramidization of the sp^2-hybridized C atoms and thus increased corrugation, results in a greater reactivity towards adsorbates when compared to graphene [43]. Further evidence of the impact that this interaction has on BL reactivity is shown in [23].

To further investigate its role in the strain-related effect observed by Raman, the BL was converted into graphene by thermally annealing monolayer GNR/BL/SiC samples in air. Consequently, monolayer GNR become bilayer thick. Figure 5 illustrates sample processing for this experiment. Raman spectroscopy was employed to investigate the edges of such type of GNRs in [23]. Results evidenced that the
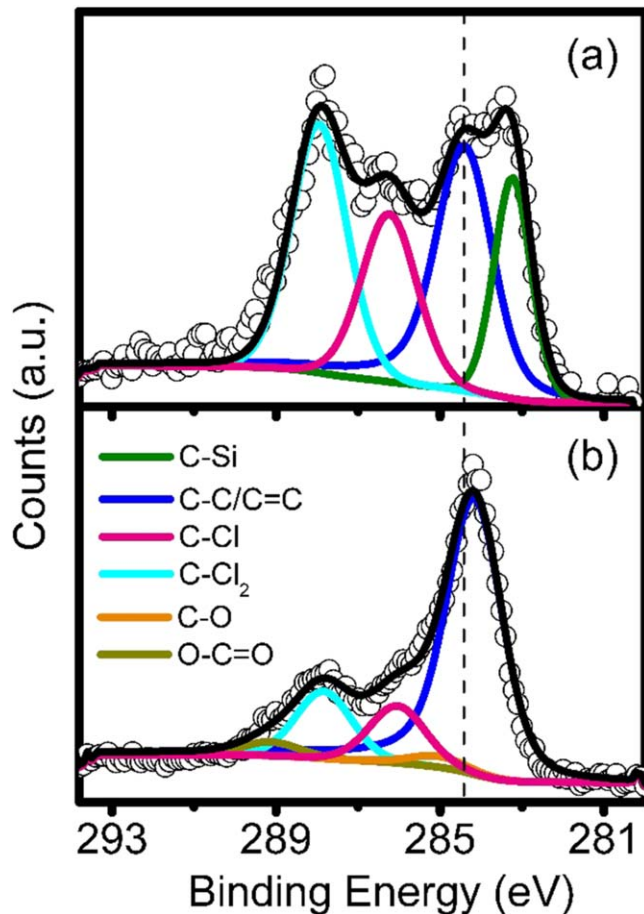
Figure 4. XPS C 1s region of (a) BL/SiC and (b) Graphene/BL/SiC after chlorination. The C–Si component does not appear in (b) due to the graphene coverage. Note that C bonded to C component shifts slightly to lower binding energies when going from BL to graphene/BL due to the larger concentration of C with sp^2 hybridization.

Figure 5. Representation of sample processing for determining BL influence on strain modifications observed in graphene after chlorination. Direct chlorination of monolayer GNR samples resulted in the incorporation of Cl in the BL (a). By annealing monolayer GNR prior to chlorination, BL is etched from areas not protected by the graphene. In covered areas, BL detaches from SiC, forming a second graphene layer. No significant strain effect was observed after the chlorination of these bilayer samples (b).

degree of disorder at these edges increases as the graphene layer propagates along the terrace during its growth. Thus, narrower bilayers GNRs offer a more ordered edge termination. The analysis also suggested that the GNRs are preferentially zigzag-terminated, following the epitaxial relation between graphene and SiC. Despite being potential incorporation sites, the observed defective edges of GNRs should not induce, at least not in the same extent, the effect produced by the BL with respect to Cl incorporation as indicated by the results of figure 4. The higher reactivity of the BL was attributed to its different atomic corrugation with respect to monolayer graphene. Differences in the average distances of BL's atoms form different sublattices results in a pyramidalization of the sp2-hybridized C atoms [44], resulting in chemical reactivity enhancement [43]. Analyzing the Raman spectra of bilayer GNR, before and after chlorination, (figure 3(b)), one can see that no significant change occurs to the 2D peak, while the G peak redshifts (figure 3(b)). It is important to point out that, in the case of the bilayer samples, bonding of Cl with SiC was detected by XPS (data not shown). Hence, the SiC surface, partially oxidized by air annealing, is able to incorporate some Cl in addition to the edges of GNRs.. However, with no BL present, no increase in

compressive strain is observed in Raman. Therefore, the strain induced to the graphene layer is likely related to the incorporation of Cl in the BL underneath. This strain modification was observed to be stable in ambient conditions over long periods of time, with the Raman spectra remaining unchanged up to 3 months after chlorination, making the stability of Cl on the BL much greater than that observed for chlorinated CVD-graphene [35].

4. Conclusions

In this work, we have demonstrated how a photochemical chlorination procedure, using Cl$_2$ gas and UV light, can be used to modify epitaxial GNR grown on SiC (0001). This technique led to the incorporation of Cl in the BL existent between graphene and the SiC substrate. The modification of the BL by chlorination resulted in induction of uniaxial compressive strain to the GNR on top, as demonstrated by Raman measurements. Techniques for applying mechanical strain to graphene such as this are much desired in band gap engineering, an essential step for enabling graphene integration to high-performance microelectronic devices.

Acknowlegments

ORCID iDs

Gabriela Copetti ⬥ https://orcid.org/0000-0003-3418-8841
Taís O Feijó ⬥ https://orcid.org/0000-0002-5336-6036
Martin Heilmann ⬥ https://orcid.org/0000-0002-5485-1244
Gabriel V Soares ⬥ https://orcid.org/0000-0002-6875-0145
Cláudio Radtke ⬥ https://orcid.org/0000-0003-3469-4920

References

[1] Geim A K and Novoselov K S 2007 *Nat. Mater.* **6** 183–91
[2] Schwierz F 2010 *Nat. Nanotechnol.* **5** 487–96
[3] Novoselov K S, Fal′ko V I, Colombo L, Gellert P R, Schwab M G and Kim K 2012 *Nature* **490** 192–200
[4] Zhang Y, Tang T-T, Girit C, Hao Z, Martin M C, Zettl A, Crommie M F, Shen Y R and Wang F 2009 *Nature* **459** 820–3
[5] Karlický F, Datta K K R, Otyepka M and Zbořil R 2013 *ACS Nano* **7** 6434–64
[6] Li H, Duan T, Haldar S, Sanyal B, Eriksson O, Jafri H, Hajjar-Garreau S, Simon L and Leifer K 2020 *Appl. Phys. Rev.* **7** 011403
[7] Jeon K-J *et al* 2011 *ACS Nano* **5** 1042–6
[8] Chronopoulos D, Bakandritsos A, Pykal M, Zbořil R and Otyepka M 2017 *Appl. Mater. Today* **9** 60–70
[9] Si C, Sun Z and Liu F 2016 *Nanoscale* **8** 3207–17
[10] Xu X, Liu C, Sun Z, Cao T, Zhang Z, Wang E, Liu Z and Liu K 2018 *Chem. Soc. Rev.* **47** 3059–99
[11] Sahalianov I Y, Radchenko T M, Tatarenko V A, Cuniberti G and Prylutskyy Y I 2019 *J. Appl. Phys.* **126** 054302
[12] Monteverde U, Pal J, Migliorato M A, Missous M, Bangert U, Zan R, Kashtiban R and Powell D 2015 *Carbon* **91** 266–74
[13] Choi S-M, Jhi S-H and Son Y-W 2010 *Nano Lett.* **10** 3486–9
[14] Son Y-W, Cohen M L and Louie S G 2006 *Phys. Rev. Lett.* **97** 089901
[15] Xu W and Lee T W 2016 *Mater. Horiz.* **3** 186–207
[16] Han M Y, Özyilmaz B, Zhang Y and Kim P 2007 *Phys. Rev. Lett.* **98** 206805
[17] Merino-Díez N, Garcia-Lekue A, Carbonell-Sanromà E, Li J, Corso M, Colazzo L, Sedona F, Sánchez-Portal D, Pascual J I and de Oteyza D G 2017 *ACS Nano* **11** 11661–8
[18] Llinas J P *et al* 2017 *Nat. Commun.* **8** 633
[19] Bennett P B, Pedramrazi Z, Madani A, Chen Y-C, de Oteyza D G, Chen C, Fischer F R, Crommie M F and Bokor J 2013 *Appl. Phys. Lett.* **103** 253114
[20] Galves L A, Wofford J M, Soares G V, Jahn U, Pfüller C, Riechert H and Lopes J M J 2017 *Carbon* **115** 162–8
[21] Lastras-Martínez L F, Almendarez-Rodríguez J, Flores-Rangel G, Ulloa-Castillo N A, Ruiz-Cigarrillo O, Ibarra-Becerra C A, Castro-García R, Balderas-Navarro R E, Oliveira M H and Lopes J M J 2017 *J. Appl. Phys.* **122** 035701
[22] Sprinkle M, Ruan M, Hu Y, Hankinson J, Rubio-Roy M, Zhang B, Wu X, Berger C and de Heer W A 2010 *Nat. Nanotechnol.* **5** 727–31
[23] Oliveira M H, Lopes J M J, Schumann T, Galves L A, Ramsteiner M, Berlin K, Trampert A and Riechert H 2015 *Nat. Commun.* **6** 7632
[24] Miccoli I, Aprojanz J, Baringhaus J, Lichtenstein T, Galves L A, Lopes J M J and Tegenkamp C 2017 *Appl. Phys. Lett.* **110** 051601
[25] Varchon F *et al* 2007 *Phys. Rev. Lett.* **99** 126805
[26] Graf D, Molitor F, Ensslin K, Stampfer C, Jungen A, Hierold C and Wirtz L 2007 *Nano Lett.* **7** 238–42
[27] Ferrari A C and Basko D M 2013 *Nat. Nanotechnol.* **8** 235–46
[28] Neumann C *et al* 2015 *Nat. Commun.* **6** 8429
[29] Lee T, Mas'ud F A, Kim M J and Rho H 2017 *Sci. Rep.* **7** 16681
[30] Mohiuddin T M G *et al* 2009 *Phys. Rev.* B **79** 205433
[31] Ferrari A C 2007 *Solid State Commun.* **143** 47–57
[32] Lee J E, Ahn G, Shim J, Lee Y S and Ryu S 2012 *Nat. Commun.* **3** 1024
[33] Mueller N S *et al* 2017 *2D Mater.* **5** 015016
[34] Bruna M, Ott A K, Ijäs M, Yoon D, Sassi U and Ferrari A C 2014 *ACS Nano* **8** 7432–41
[35] Copetti G, Nunes E H, Rolim G K, Soares G V, Correa S A, Weibel D E and Radtke C 2018 *J. Phys. Chem.* **122** 16333–8
[36] Röhrl J, Hundhausen M, Emtsev K V, Seyller T, Graupner R and Ley L 2008 *Appl. Phys. Lett.* **92** 201918
[37] Lee D S, Riedl C, Krauss B, von Klitzing K, Starke U and Smet J H 2008 *Nano Lett.* **8** 4320–5
[38] Ni Z H, Yu T, Luo Z Q, Wang Y Y, Liu L, Wong C P, Miao J, Huang W and Shen Z X 2009 *ACS Nano* **3** 569
[39] Yoon J-C, Thiyagarajan P, Ahn H-J and Jang J-H 2015 *RSC Adv.* **5** 62772–7
[40] Wang S, Suzuki S and Hibino H 2014 *Nanoscale* **6** 13838–44
[41] Frank O, Vejpravova J, Holy V, Kavan L and Kalbac M 2014 *Carbon* **68** 440–51
[42] Wang Y Y, Ni Z H, Yu T, Shen Z X, Wang H M, Wu Y H, Chen W and Wee A T S 2008 *J. Phys. Chem.* C **112** 10637–40
[43] Sclauzero G and Pasquarello A 2012 *Phys. Rev.* B **85** 161405
[44] de Lima L H, de Siervo A, Landers R, Viana G A, Goncalves A M B, Lacerda R G and Häberle P 2013 *Phys. Rev.* B **87** 081403(R)